# Unusual ligand structure in Ni–Fe active center and an additional Mg site in hydrogenase revealed by high resolution X-ray structure analysis

Yoshiki Higuchi[1]*, Tatsuhiko Yagi[2] and Noritake Yasuoka[3]

**Background:** The hydrogenase of *Desulfovibrio* sp. catalyzes the reversible oxidoreduction of molecular hydrogen, in conjunction with a specific electron acceptor, cytochrome $c_3$. The Ni–Fe active center of *Desulfovibrio* hydrogenase has an unusual ligand structure with non-protein ligands. An atomic model at high resolution is required to make concrete assignment of the ligands which coordinate the Ni–Fe center. These in turn will provide insight into the mechanism of electron transfer, during the reaction catalysed by hydrogenase.

**Results:** The X-ray structure of the hydrogenase from *Desulfovibrio vulgaris* Miyazaki has been solved at 1.8 Å resolution and refined to a crystallographic R factor of 0.229. The overall folding pattern and the spatial arrangement of the metal centers are very similar to those found in *Desulfovibrio gigas* hydrogenase. This high resolution crystal structure enabled us to assign the non-protein ligands to the Fe atom in the Ni–Fe site and revealed the presence of a Mg center, located approximately 13 Å from the Ni–Fe active center.

**Conclusions:** From the nature of the electron-density map, stereochemical geometry and atomic parameters of the refined structure, the most probable candidates for the four ligands, coordinating the Ni–Fe center, have been proposed to be diatomic S=O, C≡O and C≡N molecules and one sulfur atom. The assignment was supported by pyrolysis mass spectrometry measurements. These ligands may have a role as an electron sink during the electron transfer reaction between the hydrogenase and its biological counterparts, and they could stabilize the redox state of Fe(II), which may not change during the catalytic cycle and is independent of the redox transition of the Ni. The hydrogen-bonding system between the Ni–Fe and the Mg centers suggests the possible involvement of the Mg center in the reaction cycles of hydrogen metabolism.

Addresses: [1]Division of Chemistry, Graduate School of Science, Kyoto University, Sakyo, Kyoto 606-01, Japan, [2]Shizuoka University, 836 Oya, Shizuoka 422, Japan and [3]Department of Life Science, Faculty of Science, Himeji Institute of Technology, 1479-1 Kanaji, Kamigori, Hyogo 678-12, Japan.

*Corresponding author.
E-mail: higuchi@kuchem.kyoto-u.ac.jp

**Key words:** high resolution crystal structure, Mg center, Ni–Fe hydrogenase, pyrolysis-MS, S=O ligand

Received: **26 August 1997**
Revisions requested: **1 October 1997**
Revisions received: **23 October 1997**
Accepted: **27 October 1997**

**Structure** 15 December 1997, **5**:1671–1680
http://biomednet.com/elecref/0969212600501671

Structure  ISSN 0969-2126

## Introduction

The hydrogenase of *Desulfovibrio* sp. (EC 1.12.2.1) catalyzes the reversible oxidoreduction of molecular hydrogen in conjunction with the specific electron acceptor, cytochrome $c_3$ [1]. This enzyme has been suggested to have an ability to regulate the proton gradient between inside and outside of the periplasmic membrane, which could be involved in the system of energy metabolism of the bacteria [2]. Three types of hydrogenases, Fe only, Ni–Fe and Ni–Fe–Se hydrogenases have been found in sulfate-reducing bacteria [1]. The three-dimensional structure of the Ni–Fe hydrogenase from *Desulfovibrio gigas* was reported at 2.85 Å, showing the location, coordination and the geometry of the metal centers, and an unknown additional metal ion near the Ni atom [3]. The nature of the unknown metal was shown by anomalous dispersion to be consistent with an Fe atom. Three diatomic non-protein ligands to the Fe atom in the Ni–Fe active center, named as L1, L2 and L3, were assigned as C≡N, C≡O or N≡O based on the data of the infrared spectra in the various redox states [4]. The identity of the unusual ligands to the Fe atom was also assigned using the $^{13}$C- and $^{15}$N-enriched C≡O and C≡N by infrared spectroscopy [5,6]. To elucidate the nature of the unusual ligands to the Fe atom, we have solved the three-dimensional crystal structure of the Ni–Fe hydrogenase from *Desulfovibrio vulgaris* Miyazaki F and have succeeded in refining it at 1.8 Å resolution. Only the refined structure at high resolution X-ray analysis will enable us to obtain detailed information about the relationship between the structure and function of the active site of this hydrogenase.

The hydrogenase from the sulfate-reducing bacterium *D. vulgaris* Miyazaki F (IAM 12604) is composed of a heterodimer (62.5 and 28.8 kDa) with a molecular mass of 91 kDa [7]. The protein is homologous to the soluble hydrogenase from *Desulfovibrio gigas* [8]. It is known to have two $Fe_4$–$S_4$ clusters, one $Fe_3$–$S_4$ cluster and one Ni atom that comprise its metal centers, and recently it was found to contain an additional Fe atom near the Ni atom,

**Table 1**

**Data collection, phasing and refinement statistics*.**

| | Native | FE74 | FE73 | FE75 | NI48 |
|---|---|---|---|---|---|
| **Data collection** (Native at 1.000 Å) | | | | | |
| Resolution (Å) | 20.0–1.80 | | | | |
| No. of observed reflections | 251,414 | | | | |
| No. of unique reflections (coverage %) | 63,133 (81.3) | | | | |
| $R_{sym}$ (%)† | 4.1 | | | | |
| $R_{merge}$ (%)‡ | 10.5 | | | | |
| **Phasing** (MIR [30] + MAD)** | | | | | |
| Resolution (Å) | | 20.0–3.5 | 20.0–3.5 | 20.0–3.5 | 20.0–3.5 |
| No. of sites of anomalous scatterers refined | | 12 (11Fe + 1Ni) | 12 (11Fe + 1Ni) | 12 (11Fe + 1Ni) | 12 (11Fe + 1Ni) |
| No. of reflections (Bijvoet)†† | | 9104 (6432) | 9339 (6366) | 6443 (4453) | 7259 (5470) |
| $R_{cullis}$§ (Bijvoet)†† | | 0.87 (0.9) | 0.91 (0.8) | 0.88 (0.9) | 0.98 (0.8) |
| Phasing power | | 0.55 | 0.49 | 0.64 | 0.17 |
| $R_d$ (%)# | | 13.3 | 10.9 | 9.0 | 9.7 |
| $R_{ano}$ (%)¶ | | 7.0 | 8.2 | 6.8 | 6.2 |
| $R_{sym}$ (%)† | | 5.7 | 6.9 | 5.4 | 5.5 |
| Theoretical $\Delta f'$ ($\Delta f''$) | | | | | |
| Fe | | −9.2 (4.0) | −4.5 (3.9) | −5.3 (0.5) | −0.9 (3.0) |
| Ni | | −1.8 (0.6) | −1.8 (0.6) | −1.7 (0.6) | −7.4 (3.9) |
| **Refinement** | | | | | |
| Resolution (Å) | 6.0–1.80 | | | | |
| No. of reflections (coverage %) | 57,233 (73.7) | | | | |
| R factor (%)¥ | 22.9 ($F>\sigma(F)$) | | | | |
| No. of atoms | 6,865 | | | | |
| No. of water molecules | 638 | | | | |
| Rms bond distances (Å)‡‡ | 0.012 | | | | |
| Rms bond angles (°)‡‡ | 2.1 | | | | |
| Mean coordination error from Luzzati plot (Å) | 0.3 | | | | |

*Crystal space group is $P2_12_12_1$ with $a = 101.50$, $b = 126.50$, $c = 66.51$ Å. †$R_{sym} = (\Sigma_h\Sigma_{j=1,N} | I_j - \langle I\rangle | / \Sigma_h\Sigma_{j=1,N} I_j) \times 100$, where $I_j$ is the jth measurement of the reflection and $\langle I\rangle$ is the mean intensity of the N symmetrically related reflections. ‡$R_{merge} = (\Sigma_h\Sigma_{i=1,N} | I_i - \langle I\rangle | / \Sigma_h\Sigma_{i=1,N} I_i) \times 100$, where $I_i$ is the ith measurement of the reflection and $\langle I\rangle$ is the mean intensity of the N measurements. §$R_{Cullis}$ (for all reflections)$= \Sigma_h || F_{PH}| - |F_P + F_H|| / \Sigma_h || F_{PH}| - |F_P||$, where $F_{PH}$ is the structure factor collected at the X-rays of 1.743, 1.730, 1.750 or 1.487 Å, $F_P$ is that at 1.000 Å and $F_H$ is that of anomalous scatterers; $R_{Cullis}$ (for Bijvoet pairs) $= \Sigma_h ||| F_{PH}^+| - |F_{PH}^-|| - 2|F_H| \sin(\alpha) | / \Sigma_h || F_{PH}^+| - |F_{PH}^-||$, where $F_{PH}^+$ and $F_{PH}^-$ are Bijvoet pairs, and $\alpha$ is the phase angle of $F_P$. #$R_d = (\Sigma_h || F_{PH}| - |F_P|| / \Sigma_h |F_P|) \times 100$. ¶$R_{ano} = (\Sigma_h || F_{PH}^+| - |F_{PH}^-|| / \Sigma_h |F_{PH}|) \times 100$. ¥R factor $= (\Sigma_h | F_o - F_c | / \Sigma_h F_o) \times 100$, where $F_o$ and $F_c$ are the observed and the calculated structure factors. **The phases were obtained from MIR information at 4.0 Å [30] combined with MAD information at 3.5 Å. FE74, FE73, FE75, NI48 denote the *F*-data collected using the X-rays of 1.743, 1.730, 1.750 and 1.487 Å, respectively. The number of the sites of the anomalous scatterers (Ni and Fe) for MAD phasing was regarded as 12 (11Fe + 1Ni) because of the lack of the knowledge of the existence of additional one Fe atom near Ni site. The $\Delta f''$ values at 1.743 and 1487 Å can not be exactly estimated from the theoretical curve because of the abrupt change of the values of the imaginary part near the absorption edge of the anomalous scatterers. ††Bijvoet: statistical values for Bijvoet pairs. ‡‡Root mean square deviation from the ideal bond distances and angles calculated by the program X-PLOR [33].

creating a heterobinuclear metal center. The ready and unready states of the Ni atom have previously been investigated by EPR spectroscopy [9,10].

## Results and discussion

### Structure determination and quality of the refined model

The structure of *D. vulgaris* Miyazaki hydrogenase was determined using the techniques of multiple isomorphous replacement (MIR) and multiple anomalous diffraction (MAD) (Table 1). In the electron-density map, all of the residues in the small subunit and Ser19–His552 in the large subunit were assigned. Except for the N- and C-terminal regions of the small subunit and the N terminus of the large subunit, the temperature factors for mainchain and sidechain atoms were refined to around the mean value of 24.3 Å$^2$, and those for metal centers were well-converged to the smaller value of 13.6 Å$^2$ (Table 2). The root mean square (rms) difference of the temperature factors for the bonded atoms in the hydrogenase molecule is 2.8 Å$^2$, which is a normal valve for protein structures. There are six (two out of 31 residues in the large subunit and four out of 22 residues in the small subunit) *cis*-proline residues in the molecule. The radial distribution of the final R factor gives a mean coordination error of 0.3 Å [11]. Table 3 shows the various parameters calculated by the program PROCHECK [12] used to check

**Table 2**

**Statistics of B factors (Å²).**

| | Mean B | Rms ΔB† |
|---|---|---|
| Mainchain | 22.0 | 2.3 |
| Sidechain | 23.0 | 3.2 |
| All protein atoms | 22.5 | 2.8 |
| Ni–Fe center | 15.7 | 4.3 (3.0) |
| All metal groups* | 13.6 | 3.9 |
| $H_2O$ | 43.1 | – |
| All atoms | 24.3 | 2.8 |

*All atoms in the three iron–sulfur clusters, the Ni–Fe and the Mg centers. †Rms difference of the B values of the bonded atoms. Metal coordination bonds are included for the calculation in case of the metal centers. The value for the Ni–Fe active center of 4.3 Å² is reduced to 3.0 Å², if C≡O$^{I}$ (with an unusually big ΔB between C$^{I}$ = 13.4 Å² and O$^{I}$ = 25.4 Å²) is omitted from the calculation.

**Table 3**

**Stereochemical geometry of the refined structure of hydrogenase*.**

| | Large subunit | Small subunit |
|---|---|---|
| **Ramachandran plot** | | |
| most favored areas (%) | 88.1 | 84.1 |
| additional allowed areas (%) | 11.9 | 14.5 |
| generously allowed areas (%) | 0.0 | 0.9 |
| disallowed areas (%) | 0.0 | 0.5 |
| number of unfavored Pro and Gly (total) | 0 (71) | 2 (45) |
| **Mainchain stereochemistry** | | |
| bond lengths (% favored) | 100.0 | 99.0 |
| bond angles (% favored) | 83.9 | 86.2 |
| planarity std† (°) (6.0)‡ | 1.6 | 1.6 |
| bad contacts (%) ( 2.6)‡ | 4.7 | 2.6 |
| Cα tetrahedral distortion std† (°) (3.1)‡ | 1.7 | 2.0 |
| hydrogen bond energy std† (0.8)‡ | 0.7 | 0.8 |
| number of *cis*-proline (total) | 2 (31) | 4 (22) |
| **Sidechain stereochemistry** | | |
| number of unfavored $\chi_1$–$\chi_2$ plots (total) | 1 (296) | 2 (139) |
| $\chi_1$ torsion angles std† (°) (16.6)‡ | 16.4 | 17.2 |
| $\chi_2$ *trans* torsion angles std† (°) (19.3)‡ | 16.6 | 12.4 |
| **Total statistics** | | |
| planarity (% favored) | 86.5 | 95.5 |
| overall G factors (–0.3)‡ | 0.21 | 0.11 |

*The structure with all protein atoms and the atoms in the metal centers were checked by the program of PROCHECK [12]. †Std is the standard deviation. ‡Typical values from well-refined protein structures are given in parentheses.

the stereochemical geometry of the structure. They show that structure refinement was completed normally.

### Overall structure

The total size of one full molecule composed of a small and a large subunit is 66 × 67 × 68 Å, along the crystallographic *a*, *b* and *c* axes, respectively. The naming scheme of typical secondary structures corresponds to the hydrogenase from *D. gigas* ([3]; Figure 1a). Some regions that are shown as random coils in *D. gigas* hydrogenase can be assigned as small α helices or β strands in Miyazaki hydrogenase (Figure 1a). The mainchain folding and the structural features of the metal centers of Miyazaki hydrogenase is very similar to those of *D. gigas* hydrogenase [3] (Figure 1b), which is in accordance with their high sequence homology [8]. Two molecules can be superimposed with an rms deviation of 0.82 Å for all mainchain atoms. All of the iron–sulfur clusters are supported in the small subunit and located in the region of the subunit interface. All Fe atoms within the three iron–sulfur clusters are coordinated by sulfur atoms of cysteine residues, except for one Fe in the distal $Fe_4$–$S_4$ cluster (distantly located from Ni–Fe center) which is supported by His188. The large subunit is composed of four domains, one α-helical domain (blue in Figure 1a), two α/β-type domains, α/β$^{I}$ (green) and α/β$^{II}$ (magenta) and one β/random-coil domain (yellow). The active site, including the Ni atom and the additionally assigned Fe, is sandwiched and supported by the α/β$^{I}$ and the α/β$^{II}$ domains, and it is surrounded by the α-helical and the β/random-coil domains of the large subunit (Figure 1a).

### Ni–Fe active center

The coordination system of the Ni–Fe center of the Miyazaki hydrogenase is also very similar to that of *D. gigas* hydrogenase [3,4]. The Ni atom is coordinated by four sulfur atoms of cysteine residues (80, 84, 546 and 549). One distinct residual peak in the vicinity of the Ni atom could be assigned as an Fe atom in both dispersive ($F_{1.000Å}$–$F_{1.743Å}$) and Bijvoet ($F^{+}_{1.730Å}$–$F^{-}_{1.730}$ Å) anomalous difference Fourier maps (Figure 2). In the anomalous difference map, one can easily recognize the electron-density peaks that are roughly centered at the Fe of the iron–sulfur clusters. In the same manner, the Ni atom was also confirmed by the nickel dispersive ($F_{1.000Å}$–$F_{1.487Å}$) anomalous difference map (Figure 2). The Fe atom is coordinated by Cys84 and Cys549, which also function as the Ni ligands making the bridges between the Fe and the Ni atoms. Three distinctive electron density peaks were additionally observed in the ($2F_o$–$F_c$) map, after the Fe atom was included in the structure refinement. They stick out from the electron density of the Fe atom forming a shape like a 'coyote head', that is one big nose and two ears of nearly the same sizes (Figure 3). At the beginning of the refinement, these peaks were considered to be attributed to non-protein diatomic molecules, such as C≡O, N≡O, $N_2$ or C≡N, as in the *D. gigas* hydrogenase [3,4,13]. The ligand in the nose of the coyote corresponds to the L1 ligand, whereas the two ligands in the ears of the coyote to the L2 and L3 ligands in the *D. gigas* hydrogenase.

**Figure 1**

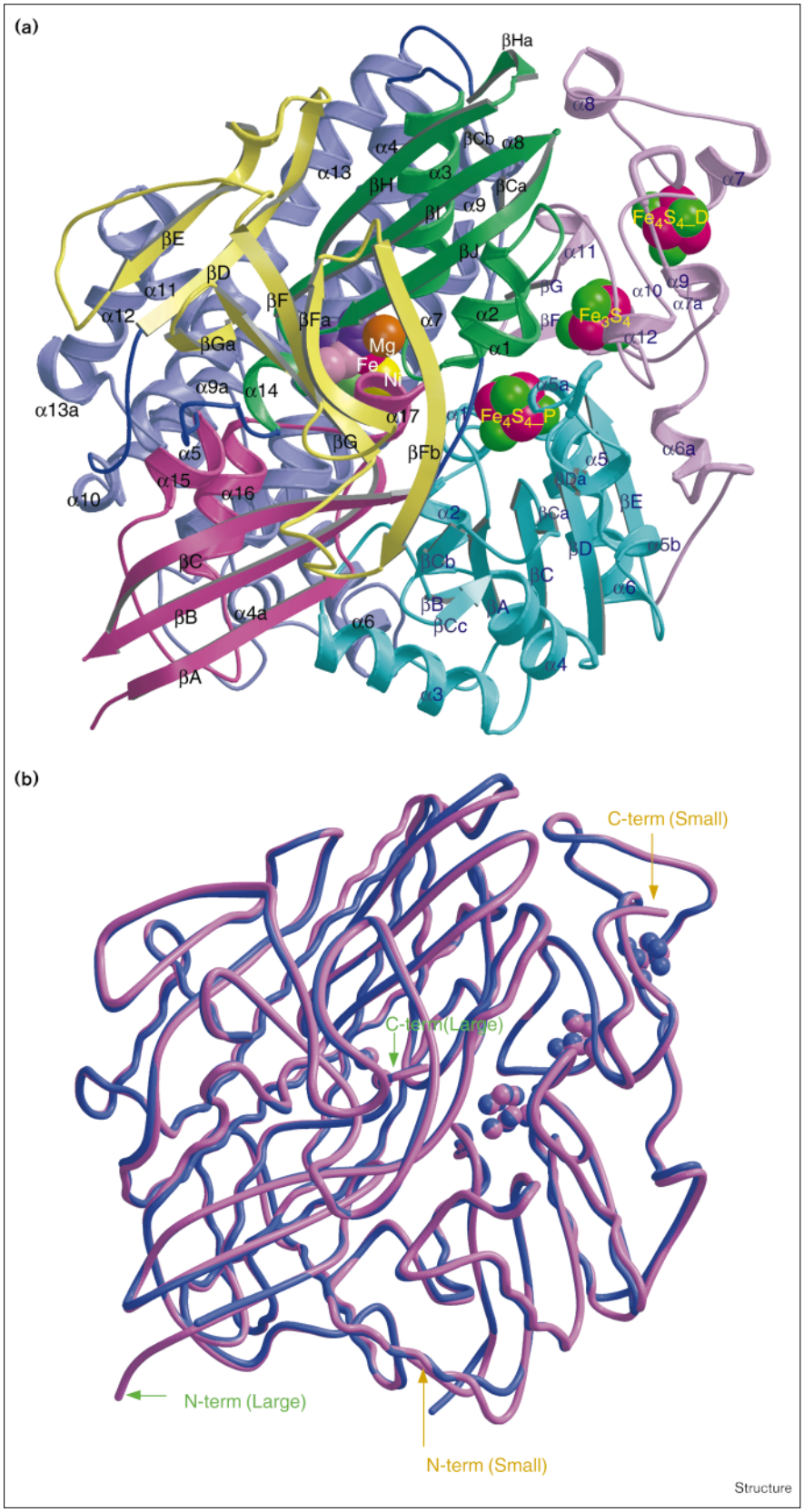


Overall structure of Miyazaki hydrogenase and comparison to *D. gigas* hydrogenase. **(a)** Schematic drawing of Miyazaki hydrogenase. The large subunit is composed of four domains, one α-helical domain composed of helices (denoted α) 4, 4a, 5, 6, 7, 8, 9, 9a, 10, 11, 12, 13a and 13, and β strands (β) Ca and Cb colored in blue; two α/β-type domains (α/β$^{I}$: with helices 15, 16 and 17, and with β strands A, B and C colored in magenta, and α/β$^{II}$: with helices 1, 2, 3 and 14, and with β strands Ha, H, I and J colored in green); and one β/random-coil domain composed of β strands D, E, Ea, F, Fa, Fb, G and Ga colored in yellow. The flavodoxin module and the remaining part of the small subunit are colored in cyan and pale pink, respectively. The metal centers are presented in balls (Fe: magenta, Ni: yellow, S=O: green, C=O or C≡N: purple and Mg: orange). The secondary structures are labeled according to the naming scheme of *D. gigas* hydrogenase [3], and additionally assigned ones are denoted by lower case letters, such as α4a, which exists between two α helices (α4 and α5). **(b)** The comparison of the mainchain folding between the Miyazaki (pink) and the *D. gigas* (blue) hydrogenases. The figure (both parts) was generated using MOLSCRIPT [36] and Raster3D [37].

**Figure 2**

Stereo view of the dispersive (in magenta) ($F_{1.000Å}$–$F_{1.743Å}$) and Bijvoet (in blue) ($F^{+}_{1.730\ Å}$–$F^{-}_{1.730\ Å}$) anomalous difference Fourier maps for the Fe atoms, and dispersive (in light green) ($F_{1.000Å}$–$F_{1.487Å}$) anomalous difference map for the Ni atom. The maps are calculated at 3.0 Å and shown at contour level of 5.0σ with ball-and-stick models shown for Ni: light green, Fe: magenta and S: green. The electron-density peaks are roughly centered at the position of the anomalous scatterers.

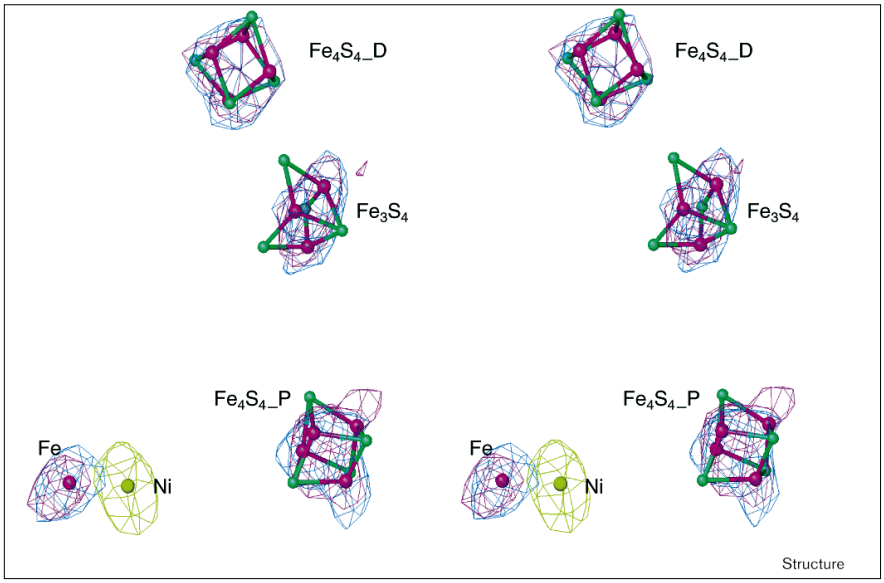


### Assignment of three diatomic ligands to the Fe atom

The coordination angle (Fe–Lp–Ld, in which Lp and Ld are the proximal and distal atoms, respectively, of the diatomic ligand to the Fe atom) for the L1 ligand is calculated to be around 170° with an approximate coordination bond distance of 2.1 Å. The molecule responsible for the density of L1 ligand was thought to be a C≡N, by considering the relatively linear bend angle that is found in the structure of *n*-butyl isocyanide bound to the heme iron of the cytochrome *c′* [14]. When a C≡N group is put in the density, however, the temperature factor of the carbon atom which is directly connected to the Fe atom had a tendency to approach to zero rapidly in the process of the structure refinement. This fact suggests that the ligand atom (Lp) in the L1 site should not be assigned as an atom such as oxygen, nitrogen or carbon atom, but it should be assigned as an atom with many more electrons, like a sulfur atom. The size of the electron density is not large enough to be ascribable to a bulky triatomic molecule, such as azide, thiocyanate, isothiocyanate or sulfur dioxide. The bond length of Lp–Ld was refined to 1.54 Å, which is exceedingly longer than ordinary C≡O or C≡N ligands to an Fe atom.

In order to clarify the molecular species in the electron density, we performed pyrolysis mass spectroscopy (MS) in

**Figure 3**

Stereo view of the omitted (Fe, Ni and ligands including cysteine residues were omitted) map (1.8 Å) in the vicinity of the Ni–Fe center contoured at 1.5σ. Two small ligands (C≡O or C≡N , currently assigned as C≡O) are fitted as the L2 and the L3 ligands, and one big ligand (S=O) as the L1 ligand. The ligand coordination geometry of the Fe atom is a slightly distorted octahedron, whereas the ligands for the Ni atom take a penta-coordinate system (square pyramid) constructed with five sulfur atoms. The atoms that comprise the Ni–Fe center are shown in ball and stick model (Fe: magenta, Ni: orange, C≡O/C≡N: blue, S=O: pink, S: violet and cysteine: green). The omitted map was calculated after the first stage of the simulated annealing refinement with four non-protein ligands.

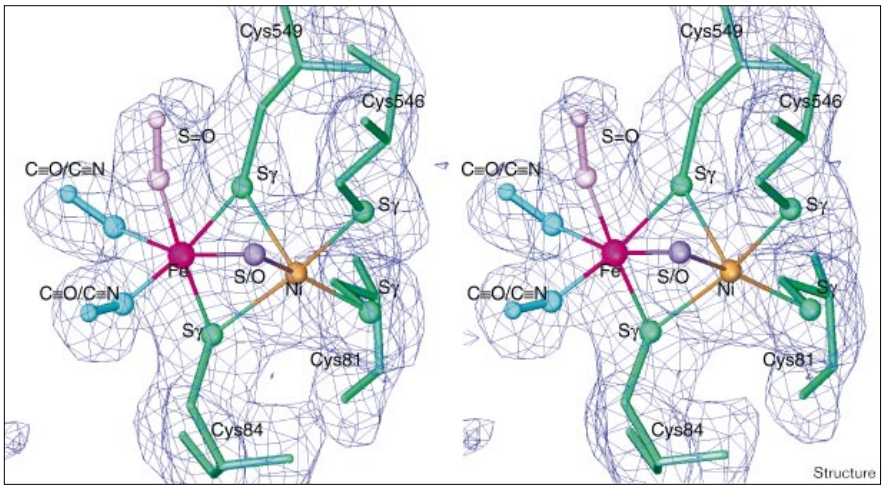

the range from 65 to 400°C. It is considered that coordination bond energy is smaller than covalent bond energy. Because the release of the ligand molecules from the Fe atom could occur at lower temperatures than those of protein pyrolysis, the ligands are expected to be distinguished from the degradation products of the protein components, if the temperature of the system is gradually raised. From the total ion chromatogram, the main peak of the protein degradation was centered at 320°C, but there are some minor peaks in the initiation period of the degradation process at 200–300°C. The mass spectrum of the gasses obtained around 220°C showed peaks at the mass numbers of 32, 33, 34, 35, 36, 48, 64, 88 and 101. The molecular species with mass numbers of 32, 33, 34, 35 and 36 have probably originated from $H_2S$ molecules, which can be considered as the degradation products of the iron–sulfur clusters. The mass numbers 48 and 64 were able to be assigned as S=O or $CH_3SH$ and $SO_2$, respectively. From the standard mass spectroscopic data, however, they should be assigned as S=O and $SO_2$ molecules [15]. A pyrolysis-MS study on a small iron–sulfur protein — ferredoxin from *Clostridium pasteurianum* — showed that there are no products belonging to the mass numbers of 48 (S=O) and 64 ($SO_2$), but that of 34 ($H_2S$) did appear in the initiation period of the protein degradation.

Taking into account of the results obtained by X-ray crystallographic and pyrolysis-MS studies, the most probable candidate for the L1 ligand is a S=O molecule. It can be considered that $SO_2$ was produced from unstable S=O molecule, during the degradation process around 200°C, because S=O is in equilibrium with $SO_2$ at high temperatures [16]. With a S=O molecule as a ligand to the Fe atom at the L1 position, the stereochemical parameters were refined as 2.11 Å (coordination bond distance), 168° (coordination angle) and B = 12.7 Å$^2$ (S), 11.8 Å$^2$ (O), at 1.8 Å resolution. These temperature factors were quite reasonable by comparison to those in the vicinity of Ni–Fe center (Ni: 18.1 Å$^2$, Fe: 13.2 Å$^2$ and S: 15.6 Å$^2$; averaged value for cysteines). The oxygen atom of the S=O can make hydrogen bonds to both the peptide N (2.91 Å) and Oγ (2.68 Å) atoms of Ser502 in the large subunit (given in parentheses are the distances between the oxygen atom of S=O and the respective atoms of Ser502). These hydrogen bonds might result in the relatively linear coordination feature of the S=O molecule to the Fe atom. Although a S=O ligand to Fe atom is unprecedented in the biomolecules, the presence of an iron complex with a S=O, two C≡O and two phenyl phosphite ligands was reported as an stable yellow crystal [17], and S=O ligands in other metal complexes is not uncommon in complex chemistry [18]. The S=O ligand to Fe is reported to be oxidized to $SO_2$ under atmospheric oxygen, but the S=O ligand in hydrogenase is buried in the protein molecule and not easily attacked by atmospheric oxygen. The frontier orbitals of S=O, which are similar in energy and size to those of C≡O, suggest that it is not impossible for the Fe-coordinating ligand to be S=O [19]. The possible nature of the S=O ligand to transition-metal atom was demonstrated and discussed by Schenk [19]. As for the biological source of S=O, a sulfoxylate ion (the hydrated species of S=O) is suggested to be an intermediate in the enzymatic reduction of bisulfite by bisulfite reductase [20]. Additional evidence for the presence of a S=O ligand by other techniques is difficult to obtain. For example, the infrared absorption band of S=O ligand to Fe atom is expected to lie between 900–1200 cm$^{-1}$ [18] with many other bands, so it will be buried in noise in ordinary infrared spectroscopy.

The coordination angles of the diatomic ligands to the Fe atom, in the L2 and the L3 positions, are calculated to be around 150°, and the coordination bond distances between the Fe and the atoms directly connected to the Fe atom are refined to be 1.8–1.9 Å. The shapes of the electron density and the coordination bond distances and angles are very similar to those of carbon monoxide which coordinates to the Fe atom of myoglobin molecule [21,22]. In infrared-spectrum of the Miyazaki hydrogenase, there are clear bands at 1955, 2080 and 2089 cm$^{-1}$. These bands can be assigned as the stretching of C≡O and C≡N bound to Fe [4,6,23]. The mass numbers of 26 (C≡N) and 28 (C≡O) were detected in the broad temperature range of the pyrolysis-MS chromatogram, but the assignment was not completed because they did not show their standard mass spectra [15]. As the initial purging process was started at 65°C, in order to avoid the adsorption of the gasses released in the process of the pyrolysis study, the C≡N and C≡O species might be released in this initial purging process. The most probable candidates in the L2 and the L3 positions are C≡O or C≡N. As X-ray crystallography cannot distinguish C≡O from C≡N ligands, two C≡O molecules, named as C≡O$^{I}$ and C≡O$^{II}$, were tentatively placed as the ligands. The coordination distances, angles and temperature factors of C≡O$^{I}$ and C≡O$^{II}$ were refined to be 1.82 Å and 1.93 Å, 152° and 154°, 13.4 Å$^2$(C$^{I}$), 25.4 Å$^2$(O$^{I}$) and 14.9 Å$^2$(C$^{II}$), 13.0 Å$^2$(O$^{II}$), respectively. The covalent bond distances between C and O atoms are 1.22 Å (C≡O$^{I}$) and 1.23 Å (C≡O$^{II}$). They are clearly smaller than the covalent bond length of the S=O bond (1.54 Å) in the L1 position. One of the oxygen atoms, O$^{II}$, hydrogen bonds to N and Nη of Arg479 of the large subunit, at distances of 3.27 Å and 3.41 Å, respectively; this could be the main reason for the large difference of the temperature factors of the oxygen atoms between the two carbon monoxides. C≡O$^{I}$ and C≡O$^{II}$ correspond to the L3 and the L2 ligands in the *D. gigas* structure, respectively. In the infrared absorption study using $^{13}$C- and $^{15}$N-enriched C≡O and C≡N, it is suggested that two C≡N and one C≡O molecules exist around the Fe atom [6]. Our assignment based on the refinement of the X-ray crystal structure suggests, however, that one of the three diatomic ligands is a S=O

molecule and therefore only two coordination sites remain for C≡N and C≡O molecules. The two possible ligand arrangements of the diatomic molecules are S=O, C≡N, C≡O or S=O, C≡O, C≡N. In order to account for the presence of two weak bands near 2080 $cm^{-1}$, we postulate that the crystalline enzyme is a mixture of two conformers differing only in microenvironment surrounding the C≡N ligand.

### The bridging ligand atom

In the initial 2.85 Å structure of *D. gigas* hydrogenase, one of six ligand positions of the Fe atom was reported to be vacant [3]. Recently, in the refined structure at a higher resolution (2.54 Å), the sixth coordination position was found to be occupied by a small electron density which was tentatively assigned to be an oxygen species for the purified hydrogenase [4]; however, the reported bond angle of 97° for Fe–O–Ni is too narrow for ordinary bond angles of bridging oxygens in binuclear metal complexes [24]. When a water oxygen atom was placed in the electron-density peak between the Ni and the Fe atoms at the initial stage of the structure refinement of Miyazaki hydrogenase, the temperature factor of the oxygen had a tendency to become less than 5.0 $Å^2$ after several cycles of the refinement. Considering the strongly hydrophobic nature of the region around the Ni–Fe center and the value of the temperature factor of the oxygen, which is unusually small, we replaced the oxygen atom with a sulfur atom and refinement cycles were repeated. The distance between the sulfur and Ni or Fe, the bond angle, Fe–S–Ni, and the temperature factor of the sulfur were refined to 2.16 Å or 2.22 Å, 71° and 19.4 $Å^2$, respectively. Although this does not exclude the possibility of an oxygen species as the bridging ligand, it remains as a second candidate to sulfur, in accordance with the atomic parameters given above. The oxygen species has been assigned as the bridging atom between Ni and Fe in the Ni–Fe hydrogenase from *D. gigas* [4], based on its kinetic data in the various redox states [25] and on the EPR Ni-signal perturbation induced by $^{17}O_2$ in the *Chromatium vinosum* hydrogenase [26]. It should be emphasized, however, that the Miyazaki hydrogenase had been purified under strict anaerobiosis and was rarely exposed to atmospheric oxygen during the crystallization [27].

### The role of the ligands in the Ni–Fe active center

The final geometry around the Ni–Fe center is shown in Table 4. The coordination geometry of the Fe atom is a slightly distorted octahedron. Considering the nature of the strong ligands and the coordination system, the Fe atom in the Ni–Fe center might be a low-spin Fe(II), even in the oxidized state. The distances between the sulfur ligands and Fe or Ni atoms are distributed in the range from 2.1 to 2.4 Å, whereas those between carbon ligands and Fe atoms are between 1.8 and 2.0 Å. On the other hand, the Ni atom is in a penta-coordinate system (square pyramid), constructed by five sulfur ligands. The statistics of the temperature factors are summarized in the Table 2. The mean value of the temperature factors of the atoms in the Ni–Fe active center is calculated to be 15.7 $Å^2$ . This

**Table 4**

**Geometry of the Ni–Fe active center of Miyazaki hydrogenase.**

**Coordination distances and angles (Fe–Ni distance = 2.55 Å)**

| Lp* Geometry | S(S=O) | C(C≡O$^{I}$) | C(C≡O$^{II}$) | S | | S(Cys549) | S(Cys84) | S(Cys81) | S(Cys546) |
|---|---|---|---|---|---|---|---|---|---|
| Fe–Lp† (Å) | 2.11 | 1.82 | 1.93 | 2.22 | | 2.37 | 2.14 | – | – |
| Fe–Lp–Ld‡ (°) | 168 | 152 | 154 | 71§ | | 120 | 105 | – | – |
| Ni–Lp† (Å) | – | – | – | 2.16 | | 2.37 | 2.38 | 2.22 | 2.33 |
| Ni–Lp–Ld‡ (°) | – | – | – | – | | 116 | 117 | 93.4 | 120 |

**Angles around the Metals (Lp1–M–Lp2)**

| Lp1¶ | S(S=O) | C(C≡O$^{I}$) | C(C≡O$^{II}$) | S | S(Cys549) | S(Cys549) | S(Cys84) | S(Cys81) | S(Cys546) |
|---|---|---|---|---|---|---|---|---|---|
| | Angles around Fe (Lp1–Fe–Lp2)(°) | | | | | Angles around Ni (Lp1–Ni–Lp2)(°) | | | |
| Lp2¶ | | | | | | | | | |
| C(C≡O$^{I}$) | 82.6 | – | – | – | – | – | – | – | – |
| C(C≡O$^{II}$) | 85.0 | 85.5 | – | – | – | – | – | – | – |
| S | 74.7 | 157 | 95.4 | – | – | 91.1 | 94.6 | 153 | 70.5 |
| S(Cys549) | 91.4 | 87.8 | 173 | 89.7 | – | – | 83.3 | 113.2 | 96.5 |
| S(Cys84) | 175 | 103 | 95.5 | 99.8 | 88.7 | – | – | 99.1 | 165 |
| S(Cys81) | – | – | – | – | – | – | – | – | 94.8 |

*Lp is the Ligand atom that directly bonds to the metal. †Coordination distance between the metal and the ligand atom (Lp). ‡Coordination angle of Fe(Ni)–Lp–Ld, where Ld is the atom in ligand which bonds to Lp. §This bond angle is defined by Ni–S–Fe. ¶Lp1 and Lp2 are ligand atoms which directly bond to the metal (Fe or Ni).

**Figure 4**

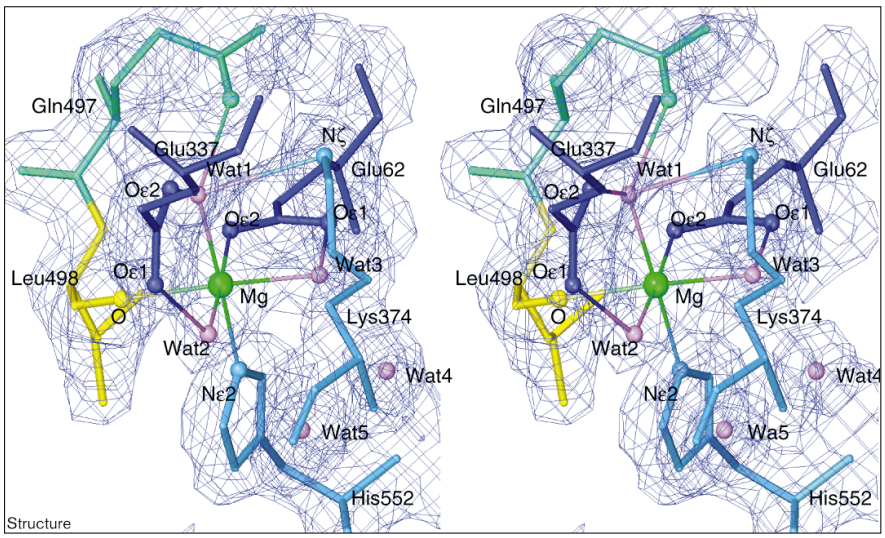


Stereo view of the $2F_o–F_c$ electron-density map (1.8 Å) around the Mg atom contoured at 1.5σ with a ball-and-stick model of the ligands (Mg: green, Glu: purple, Gln: cyan, Leu: yellow, Arg, Lys, His: sky-blue and Wat: pink). The ligands to the metal are the Nε2 atom of the imidazole ring of His552, the oxygen atom (Oε2) of the sidechain of Glu62, the carbonyl oxygen of Leu498 and three water oxygen molecules, Wat1, Wat2 and Wat3, which are further hydrogen bonded by Oε1 and Oε2 of Glu337 and Oε1 of Glu62, respectively. There exist various hydrogen-bonding networks including some sidechain atoms and water molecules.

value is distinctly smaller than that of 22.5 Å$^2$ for all protein atoms. The rms difference of B factor of the bonded atoms in the Ni–Fe active center is 4.3 Å$^2$. The value is similar to that for all metal groups, but slightly larger than that for all bonded protein atoms (2.8 Å$^2$). This large value is caused by the big difference of the B factors between C$^I$ (13.4 Å$^2$) and O$^I$ (25.4 Å$^2$) in the L3 position — when the C≡O$^I$ was omitted from the calculation, the value was reduced to 3.0 Å$^2$, which is similar to the value for all bonded atoms (2.8 Å$^2$). The temperature factors of the atoms in the Ni–Fe center were well-converged, despite the presence of the novel non-protein ligands that were assigned in the coordination sites.

The data obtained for the hydrogenase from *Chromatium vinosum* from infrared and EPR spectroscopic studies suggest that the hydrogen-activating center is localized near the Ni atom [5]. By taking account of the three-dimensional structure at high resolution, however, it is plausible to consider that all of four ligands could be involved and possess a key role in hydrogen metabolism. The electron densities around the bonds between Fe and C≡O (or C≡N) or S have hour-glass features, whereas that around the bond between the Fe and S=O is evenly strong throughout (Figure 3). This unusual structural motif around the Ni–Fe center, including the hydrogen-bonding network with surrounding amino acids, suggests that one rather stable ligand (S=O) and three slightly unstable ligands (C≡N, C≡O and S) cooperatively participate in the redox reaction of dihydrogen molecule. One or some of the ligands might have a function as an electron sink during the two-electrons reaction of hydrogen metabolism. The structural relationship between hydrogenases and other Ni–Fe enzymes, such as carbon monoxide dehydrogenases, should be an interesting topic for future study.

### The Mg atom in the C terminus of the large subunit

The C terminus of the large subunit in the crystal structure of Miyazaki hydrogenase is His552, which is completely buried in the molecule as in *D. gigas* hydrogenase [3]. There remains no space to extend the molecule downstream of His552 to include the residues observed in the DNA sequence [8]. It can be easily understood that this is caused by functional maturation of the large subunit by cleavage of the last 15 residues as proposed by Menon *et al.* [28]. The imidazole ring of His552 is stabilized by hydrogen bonding to an atom located in one large peak, which is surrounded by another five electron-density peaks (Figure 4). In the structure of *D. gigas* hydrogenase determined at 2.85 Å resolution [3], this big electron-density peak was assigned as a water oxygen. In the structure of Miyazaki hydrogenase at 1.8 Å resolution, however, it has been found that the peak was coordinated in the shape of an almost regular octahedron. The distances between ligand atoms and the atom that is responsible for this electron density are distributed in the range from 2.1 to 2.3 Å. The ligand atoms that participate in the coordination to this peak are the Nε2 atom of the imidazole ring of His552 the Oε2 atom of the sidechain of Glu62, the carbonyl oxygen of Leu498 and three water oxygen molecules, Wat1, Wat2 and Wat3, which are further hydrogen bonded by Oε1 and Oε2 of Glu337 and Oε1 of Glu62, respectively. In addition, various hydrogen-bonding networks, including some sidechain atoms and water molecules, exist. From the measurements of inductively coupled plasma atomic emission spectroscopy (ICP-AES), it has been found that Miyazaki hydrogenase contains 0.4 Mg relative to 1.0 Ni or 12.6 Fe. The results from the ICP-AES spectrum indicate that a Mg atom is the most probable candidate for the additional electron density located in the C terminus of the large subunit. In fact, when an

oxygen atom was assigned to this peak, its temperature factor was refined to a minimum value (2.0 Å$^2$), but after replacing the oxygen with Mg, the temperature factor of this atom converged to 5.6 Å$^2$. This tendency indicates that the value of the temperature factor of each atom of the Miyazaki hydrogenase after refinement is sufficiently reliable. The role of the Mg atom is now unclear. Because the Mg atom is not located on the same side of the Ni–Fe center (approximately 13 Å apart from the Ni–Fe center) as the iron–sulfur clusters in the small subunit, it is unlikely that the Mg atom is directly involved in the electron-transfer system. The sidechain atom (Nδ1) of one of its ligand residue, His552, however, is hydrogen bonded to the mainchain carbonyl oxygen atom of the Cys549, which makes a bridge between the Ni and the Fe atoms. This feature suggests that the Mg center might be involved in not only the process of the cleavage of the C terminus of the large subunit and the stability of the structure, but also in the reactions of hydrogen metabolism, such as proton transfer system.

## Biological implications

**The hydrogenase of *Desulfovibrio* sp. catalyzes the reversible oxidoreduction between molecular hydrogen and a specific electron acceptor, cytochrome $c_3$. A high resolution atomic model of hydrogenase is required to identify the ligands which coordinate the Ni–Fe center, and to subsequently understand the mechanism of electron transfer in hydrogen metabolism. On the basis of the refined crystal structure of the Ni–Fe hydrogenase from *Desulfovibrio vulgaris* Miyazaki F at a high resolution (1.8 Å), three diatomic ligand species coordinating the Fe atom in the Ni–Fe active center have been proposed to be S=O, C≡O and C≡N, and a sulfur atom has been postulated to be the bridging ligand between the Ni and the Fe atoms. These assignments are supported by the data from pyrolysis mass spectroscopy and infrared spectroscopy. The non-protein ligands to the Fe atom should cooperatively participate in the system of hydrogen metabolism, for example, as an electron sink during the electron-transfer reaction between the hydrogenase and the biological electron carrier protein, cytochrome $c_3$. Another possible role of these ligands might be to stabilize the redox state of Fe(II), which may not change during the catalytic cycle and is independent of the redox transition of the Ni. Although a S=O ligand in protein molecule is unprecedented, it has been chemically synthesized and intensively studied in small inorganic complexes, and could it be a candidate for a biomimetic hydrogen active center. The possible presence of a S=O ligand calls attention to the sulfur metabolism including the biosynthesis, transfer and incorporation of S=O molecules into protein molecules in the living cell.**

**The existence of an additional Mg site close to the Ni–Fe center is also very interesting, because it too may have a role in hydrogen metabolism and could also contribute to the stability of the active center. The site-directed mutagenesis of the amino acids which coordinate the Mg atom will be a most interesting topic for future study of this enzyme. These results suggest the necessity of high resolution crystal structure analyses, even for biomolecules of high molecular weight.**

## Materials and methods

*Structure analysis*

The X-ray structure analysis has been done on the soluble portion of *D. vulgaris* hydrogenase isolated and purified, under strict anaerobiosis throughout, from periplasmic membrane by trypsin digestion; this portion maintains more than 90% of the hydrogenase activity of the native molecule [7] Hydrogenase crystals were obtained by the sitting-drop vapor diffusion method [27] and were sealed in thin capillary tubes under the atmosphere of argon. All X-ray diffraction data were collected with the use of a Weissenberg camera for macromolecular crystallography [29] installed at the BL-6A beam station of the Photon Factory, National Laboratory for High Energy Physics in Tsukuba, Japan (Table 1). The molecular structure was determined independently of the *D. gigas* hydrogenase structure at atomic resolution by the multiple isomorphous replacement method at 4.0 Å (on five heavy-atom derivatives of ethyl mercury thiosalicylate, $K_3UO_2F_5$, $K_3IrCl_6$, $K_2PtCl_6$ and uranyl acetate) [30] combined with the multiwavelength anomalous diffraction data (1.487, 1.730, 1.743 and 1.750 Å) from a single native crystal at 3.5 Å resolution. Data statistics of the MIR and MAD experiments were shown in the previous report [30]. The number of the sites of the anomalous scatterers (Ni and Fe) for MAD phasing was regarded as 12 (11Fe+1Ni) because of the lack of the knowledge of the existence of additional one Fe atom near the Ni site. The location of the Fe atoms in the iron–sulfur clusters (orientation of the iron–sulfur clusters) were deduced from the connecting features with the ligand atoms. The model building was started using the electron density map at 4.0 Å resolution. The starting electron-density map was not in good quality, but the MIR+MAD phases at 3.5 Å were improved by iterative solvent flattening and histogram mapping with the program DM [31]. The mainchain model was built into this map, and the molecular envelope was re-estimated using the backbone model with the program MAMA in CCP4 [31]. The map was further improved by solvent flattening and phases were extended to 3.0 Å resolution. The final model building was done in this map at 3.0 Å resolution using O [32]. The model (Leu1–Asn267 of the small subunit, Ser19–His552 of the large subunit, metal centers and 638 ordered water molecules with reasonable temperature factors) was refined to an R factor of 0.200 for 47,223 reflections ($F > 3\sigma$) at the resolution 6.0 to 1.8 Å with X-PLOR [33]. Throughout the refinement, the parameter set files of parahcsdx.pro by Engh and Huber [34] and the modified parameters for the metal cluster in the X-PLOR manual [33] were used for the amino acid residues and iron–sulfur clusters, respectively, whereas the restraints for the ligand molecules were reduced to 40% of those applied to the metal (iron–sulfur) clusters. Individual atomic B factor refinement was carried out using the restraints placed on the B factors between atoms forming bonds and angles. The R factor for the final refined model to 1.8 Å for 57,233 important reflections ($F > \sigma$) was 0.229 (Table 2). During the refinement free R factor [35] was dropped from 0.475 to 0.278 for 7% of the total reflections.

*Spectroscopy of the non-protein ligands and chemical analysis of the metals*

The chemical analysis has been done by Toray Research Center in Shiga and Matsushita Technoresearch, Inc., in Osaka, Japan. The protein sample was isolated and purified [27] and dialyzed against pure water. For the pyrolysis study, the protein was freeze-dried after dialysis. The analysis of the metal atoms was performed by inductively coupled plasma atomic emission spectroscopy (ICP-AES). The hydrogenase solution contained 277 ± 1 μg Fe, 23.1 ± 0.3 μg Ni, 3.87 ± 0.001 μg

Mg, 1.02 ± 0.0006 μg Ca and 0.15 ± 0.02 μg Co. The data showed that hydrogenase contains 12.6 Fe, 0.4 Mg, 0.06 Ca and 0.006 Co relative to 1.0 Ni. The nature of the ligands to the Fe atom in the Ni–Fe center was studied by pyrolysis-mass spectroscopy (MS) and infrared spectroscopy. For pyrolysis-MS study the starting temperature was set at 65°C and temperature was raised to 400°C at the rate of 10°C/min. The released gasses were directly introduced to electron ionization (EI)-spectrometer. For the measurement of infrared spectroscopy, the protein sample was concentrated to 1.0 mM. The measurement was performed for the isolated hydrogenase in infrared-transmittance cell with CaF2 windows and Teflon spacers of 50 μm at 25°C in air. The spectrum was averaged 512 scans at 2.0 $cm^{-1}$ resolution.

### *Accession numbers*

Atomic coordinates of the structure have been submitted to the Brookhaven Protein Data Bank with the accession code 1H2A.

## Acknowledgements

We are indebted to K Miki, T Shono, S Misaki, Y Morimoto, K Fujimoto, T Okamoto and Y Iga for their helpful discussions and technical advice. We acknowledge JC Fontecilla-Camps, M Frey and A Volbeda for their kindly sending the coordinates of the *D. gigas* hydrogenase for the comparison between two structures. This work has been supported in part by a grant from the Ministry of Education, Science and Culture of Japan (no. 08458209), from New Energy and Industrial Technology Development Organization (NEDO) / Research Institute of Innovative Technology for The Earth (RITE) and from Hyogo Science and Technology Association (The program for Encouragement of Young Scientists) for which the authors express their sincere thanks.

## References

1. Yagi, T. (1988). Hydrogenase. In *Metalloproteins, Chemical Properties and Biological Effects*. (Otsuka, S., & Yamanaka, T., eds), pp. 229–244, Kodansha/Elsevier, Tokyo/Amsterdam.
2. Peck, H.D., Jr. & LeGall, J. (1982). Biochemistry of dissimilatory sulphate reduction. *Phil. Trans. R. Soc. Lond. B* **298**, 443–446.
3. Volbeda, A., Charon M.-H., Piras, C., Hatchikian, E.C., Frey, M. & Fontecilla-Camps, J.C. (1995). Crystal structure of the nickel–iron hydrogenase from *Desulfovibrio D. gigas*. *Nature* **373**, 580–587.
4. Volbeda, A., *et al*., & Fontecilla-Camps, J.C. (1996). Structure of the [NiFe] hydrogenase active site: evidence for biologically uncommon Fe ligands. *J. Am. Chem. Soc.* **118**, 12989–12996.
5. Van der Spek, T.M., *et al*., & Albracht, S.P.J. (1996). Similarities in the architecture of the active sites of Ni-hydrogenases and Fe-hydrogenases detected by means of infrared spectroscopy. *Eur. J. Biochem.* **237**, 629–634.
6. Happe, R.P., Roseboom, W., Pierik, A.J., Albracht, S.P.J. & Bagley, K.A. (1997). Biological activation of hydrogen. *Nature* **385**, 126.
7. Yagi, T., Kimura, K., Daidoji, H., Sakai, F., Tamura, S. & Inokuchi, H. (1976). Properties of purified hydrogenase from the particulate fraction of *Desulfovibrio vulgaris*, Miyazaki. *J. Biochem.* **79**, 661–671.
8. Deckers, H.M., Wilson, F.R. & Voordouw, G. (1990). Cloning and sequencing of a [NiFe] hydrogenase operon from *Desulfovibrio vulgaris* Miyazaki F. *J. Gen. Microbiol.* **136**, 2021–2028.
9. Asso, M., Guigliarelli, B., Yagi, T. & Bertrand, P. (1992). EPR and redox properties of *Desulfovibrio vulgaris* Miyazaki hydrogenase: comparison with the Ni–Fe enzyme from *Desulfovibrio gigas*. *Biochim. Biophys. Acta.* **1122**, 50.
10. Geßner, C., Trofanchuk, O., Kawagoe, K., Higuchi, Y., Yasuoka, N. & Lubitz, W. (1996). Single crystal EPR study of the Ni center of NiFe hydrogenase. *Chem. Phys. Lett.* **256**, 518–524.
11. Luzzati, P.V. (1952). Traitement statistique des erreurs dans la determination des structures cristallines. *Acta Cryst.* **5**, 802–810.
12. Laskowski, R.A., MacArthur, M.W., Moss, D.S. & Thornton, J.M. (1994). PROCHECK: a program to check the stereochemical quality of protein structures. *J. Appl. Cryst* **26**, 283–291.
13. Fontecilla-Camps, J.C. (1996). The active site of Ni–Fe hydrogenases: model chemistry and crystallographic results. *J. Biolog. Inorg. Chem* **1**, 91–98.
14. Tahirov, T.H., *et al*., & Yasuoka, N. (1996). Concerted movement of sidechains in the haem vicinity observed on ligand binding in cytochrome *c′* from *Rhodobacter capsulatus*. *Nat. Struct. Biol.* **3**, 459–464.
15. McLafferty, F.W. & Stauffer D.B. (1983). *The Wiley/NBS Registry of Mass Spectral Data,* Vol.1, pp. 2–6, John Wiley & Sons, New York.
16. Bitterer, H. (1980). In *Gmelin handbuch der Anorganischen Chemie, Ergänzungsband 3, Schwefeloxide.* (Bitterer, H., Hasse, V., Hebel, B., Kirschstein, G. & Wagner, J., eds), pp. 40, Springer-Verlag, Berlin.
17. Lorenz I.P., Hiller, W. & Conrad, M. (1985). Nukleophile substitution an thionyl- und sulfurylchlorid mit metallaten. Synthese und struktur der $SO^-$ bzw–$SO_2^-$ komplexe $[C_6H_5O_3P_2](CO)_2Fe(SO_n)$(n=1,2). *Naturforsch B* **40**, 1383–1389.
18. Polak, M.L., Fiala, B.L., Ervin, K.M. & Lineberger, W.C. (1991). The ultraviolet photoelectron spectrum of $SO^-$. *J. Chem. Phys.* **94**, 6926–6927.
19. Schenk, W.A. (1987). Sulfur oxides as ligands in coordination compounds. *Angew. Chem. Int. Ed. Engl.* **26**, 98–109.
20. Kobayashi, K., Seki, Y. & Ishimoto, M. (1974). Biochemical studies on sulfate-reducing bacteria. XIII. sulfite reductase from *Desulfovibrio vulgaris*: mechanism of trithionate, thiosulfate, and sulfide formation and enzymatic properties. *J. Biochem* **75**, 519–529.
21. Quillin, M.L., Arduini, R.M., Olson, J.S. & Phillips, G.N., Jr. (1993). High-resolution crystal structures of distal histidine mutants of sperm whale myoglobin. *J. Mol. Biol.* **234**, 133–154.
22. Schlichting, I., Berendzen, J., Phillips, G.N. & Sweet, R.M. (1994). Crystal structure of photolysed carbonmonoxy-myoglobin. *Nature* **371**, 808–812.
23. Bagley, K.A., Duin, E.C., Roseboom, W., Albracht, S.P.J. & Woodruff, W.H. (1995). Infrared-detectable groups sense changes in charge density on the nickel center in hydrogenase from *Chromatium vinosum*. *Biochemistry* **34**, 5527–5535.
24. Wilkinson, G., Gillard, R.D. & McCleverty, J.A. (1987). Comprehensive coordination chemistry. In *The Synthesis, Reactions, Properties and Applications of Compounds*. (Wilkinson, G., Gillard, R.D. & McCleverty, J.A., ed), vol. 2, pp. 301, Pergamon Press, Oxford.
25. Fernandez, V.M., Hatchikian, E.C. & Cammack, R. (1985). Properties and reactivation of two different deactivated forms of *Desulfovibrio gigas* hydrogenase. *Biochim. Biophys. Acta* **832**, 69–79.
26. van der Zwaan, J.W., Coremans, J.M.C.C., Bouwens, E.C.M. & Albracht, S.P.J. (1990). Effect of $^{17}O_2$ and $^{13}CO$ on EPR spectra of nickel in hydrogenase from *Chromatium vinosum*. *Biochim. Biophys. Acta.* **1041**, 101–110.
27. Higuchi, Y., *et al*., & Inokuchi, H. (1987) . Single crystals of hydrogenase from *Desulfovibrio vulgaris* Miyazaki F. *J. Biol. Chem.* **262**, 2823–2825.
28. Menon, N.K., *et al*., & Przybyla, A.E. (1993). Carboxy-terminal processing of the large subunit of [NiFe] hydrogenases. *FEBS Lett.* **331**, 91–95.
29. Sakabe, N. (1991). X-ray diffraction data collection system for modern protein crystallography with a Weissenberg camera and an image plate using synchrotron radiation. *Nucl. Instrum. Methods. Phys. Res. A* **303**, 448–463.
30. Higuchi, Y., *et al*., & Yasuoka, N. (1994). Location of active sites of NiFe hydrogenase determined by the combination of multiple isomorphous replacement and multiwavelength anomalous diffraction methods. *Acta Cryst* D **51**, 553–555.
31. SERC Daresbury Laboratory. (1979). CCP4: a suite of programs for protein crystallography. Warrington, UK.
32. Jones, T.A., Zou, J.Y., Cowan, S.W. & Kjeldgaard, M. (1991). Improved methods for binding protein models in electron density maps and the location of errors in these models. *Acta Cryst* A **47**, 110–119.
33. Brünger, A.T. (1992). *X-PLOR, Version 3.1, A System for X-ray Crystallography and NMR*. Yale University Press, New Haven, CT.
34. Engh, R.A. & Huber, R. (1991). Accurate bond and angle parameters for X-ray protein-structure refinement. *Acta Cryst. A* **47**, 392–400.
35. Brünger, A.T. (1992). The free R value: a novel statistical quantity for assessing the accuracy of crystal structures. *Nature* **355**, 472–474.
36. Kraulis, P.J. (1991). MOLSCRIPT: a program to produce both detailed and schematic plots of protein structures. *J .Appl. Cryst* **24**, 946–950.
37. Merrit, E.A. & Murphy, M.E. (1994). Raster3D Version 2.0: a program for photorealistic molecular graphics. *Acta Cryst D* **50**, 869–873.